Electrical Engineering
https://doi.org/10.1007/s00202-019-00867-w

ORIGINAL PAPER

Eliminating the effect of hot spots on underground power cables using cool pavements

Dardan Klimenta[1] · Dragan Tasić[2] · Bojan Perović[1] · Jelena Klimenta[3] · Miloš Milovanović[1] · Ljiljana Anđelković[1]

Received: 27 June 2019 / Accepted: 24 October 2019

Abstract

It is well known that hot spots limit the ampacities of underground power cables. There are many commonly applied methods to control the thermal environment in hot spots of underground power cables. However, applications of cool pavements for this specific purpose would be a novelty in the field of power cable engineering. This paper considers the use of different cool pavements in combination with thermally stable bedding and/or pure quartz sand for mitigating or eliminating the thermal effect of an actual hot spot on the ampacities of a 110 kV cable line and a group of four 35 kV three-core cables installed in Belgrade, the Republic of Serbia. In the hot spot, the 110 kV cable line is installed in parallel with the group of 35 kV cables and crosses a district heating pipeline. All distances between these underground installations are lower than the recommended ones, and the 110 kV and 35 kV cables are laid at depths greater than required. The mutual thermal effects between the underground installations in the hot spot are simulated using FEM-based models for different environmental conditions. An experimental background is also provided. In comparison with the corresponding base cases, it has been found that the ampacities of the 110 kV cable line and group of 35 kV cables can be increased up to 25.1% and 60.9% in summer, and up to 62.8% and 170% in winter, respectively.

Keywords Ampacity · Cool pavement · Finite element method (FEM) · Hot spot · Power cable · Thermal effect

List of symbols

Variables and coefficients

d_c	Conductor diameter (m)
h	Heat transfer coefficient due to convection [W/(m^2 K)]
I	Load current (A)
I_{cp}	Cable ampacity (A)
k	Thermal conductivity [W/(m K)]
n	Length of the normal vector $\vec{n}$ (m)
$Q_{S,s}$	Solar irradiance incident on the earth surface (W/m^2)
Q_v	Volume power of heat sources (W/m^3)
q_0	Specified heat flux on the upper surface of the heating-pipe duct (W/m^2)
R_{ac}	Effective conductor resistance to the flow of alternating current, i.e. effective a.c. resistance (Ω/m)
S'_c	Geometric cross-sectional area of conductor (m^2)
T	Unknown temperature or unknown surface temperature (K)
T_a	Temperature of the air contacting the earth surface (K or °C)
$T_{c,max}$	Temperature of the most thermally loaded conductor (°C)
T_{cp}	Continuously permissible temperature of cables (°C)
v_a	Wind velocity (m/s)

✉ Dardan Klimenta
dardan.klimenta@pr.ac.rs

Dragan Tasić
dragan.tasic@elfak.ni.ac.rs

Bojan Perović
bojan.perovic@pr.ac.rs

Jelena Klimenta
klimenta.jelena@gmail.com

Miloš Milovanović
milos.milovanovic@pr.ac.rs

Ljiljana Anđelković
ljiljana.andjelkovic@pr.ac.rs

[1] University of Priština in Kosovska Mitrovica, Kosovska Mitrovica, Serbia

[2] University of Niš, Niš, Serbia

[3] ProElectric SD, Kraljevo, Serbia

Published online: 08 November 2019

x, y	Cartesian spatial coordinates (m)
α	Solar absorptivity (dimensionless)
ε	Thermal emissivity (dimensionless)
σ_{SB}	Stefan–Boltzmann constant [W/(m^{2}K^4)]

Abbreviations

2D and 3D	Two-dimensional and three-dimensional
EUR and €	National currency of the European Union member states
FEM	Finite element method
HDPE	High-density polyethylene
NA2XS(FL)2Y	Single-core power cable, N—standardised/norm type, A—aluminium conductor, 2X—cross-linked polyethylene insulation, S—copper screen, FL—longitudinally and crosswise water-tight, and 2Y—polyethylene outer sheath
NAEKEBA	Three-core power cable, N—standardised/norm type, A—aluminium conductor, EK—metal sheath of lead with corrosion protection on each sheath, E—thermoplastic sheath and inner protective covering, lapped bedding with additional layer of plastic tape, B—armour of steel tape, and A—outer protection of fibreous material (jute) in compound
PE	Polyethylene
PQS	Pure quartz sand
SI	International System of Units
TSB	Thermally stable bedding
XLPE	Cross-linked polyethylene

1 Introduction

Conventional methods for increasing the ampacity of underground power cables are the following: special cable beddings, systems for forced cooling, and systems for irrigation. In addition, some other methods, such as cool pavements, can be used for the same purpose [1]. According to [1], each of these methods should be applied on the entire route of an underground cable line. Moreover, the conventional methods have long been used to control the thermal environment in hot spots of underground power cables and there are prescribed guidelines and procedures for their application. However, unconventional methods such as cool pavements have not yet been applied in any hot spot of an underground cable line. Accordingly, the mitigation or elimination of the hot spot effect on the cable ampacity using the cool pavements can be regarded as a novelty in the field of power cable engineering.

In connection with the unconventional methods, there are several research papers [1–6] that concern only the control of the thermal environment of underground power cables in accordance with the general requirements for the design and installation [7, 8]. In particular, all these papers did not deal with the mitigation or elimination of the hot spot effect.

Otherwise, there are a large number of research papers dealing with hot spots and conventional methods, as is the case with book [9] which is one of the most cited publications in the field. However, in most of these papers, as well as in [9], the effect of the solar heating on underground power cables is not included, the FEM is not applied according to [8], cases where the cable trenches are completely filled with bedding material are not analysed and the effects of the radiation properties of the surface of the soil or pavement above the cables are not taken into account. As far as the authors are concerned, along with the papers of Klimenta et al. [1–6], the effect of the solar heating on underground power cables was only considered in the studies of Nahman and Tanasković [10–12], Terracciano et al. [13], Yang et al. [14], and Lindström [15].

In this paper, an actual hot spot from [16] is considered, consisting of three single-core 110 kV cables in the first cable trench, four three-core 35 kV cables in the second cable trench, and a heating pipeline placed at a non-standard distance below the cables. The cables are parallel to each other, installed at a depth of 2.121 m (instead of 1.2–1.5 m and 1 m for the 110 kV and 35 kV cables [7, 17], respectively) and perpendicular to the heating pipeline. In addition, the minimum separation distance for right angle crossing between the 110 kV or 35 kV cables and the heating pipeline is 1 m. The 110 kV line consists of cables of the type NA2XS(FL)2Y $1\times1000/95$ mm^2 64/110 kV, and the four 35 kV cables are of the type NAEKEBA 3×150 mm^2 20/35 kV. In contrast to the paper [16] dealing with a nonlinear dynamic thermal analysis of the hot spot, a nonlinear steady-state thermal analysis of the same hot spot is carried out in this paper. The analysis is performed using the FEM-based simulation software COMSOL Multiphysics [18], whose resources are significantly larger in terms of the type of thermal analysis.

The aim of this paper is to show how cool pavements in combination with thermally stable bedding and/or pure quartz sand can mitigate or eliminate negative thermal effects of an actual hot spot on the cable ampacities. In order to achieve this, the following was necessary:

- To assume (i) that three phase loads in the 110 kV circuit are mutually equal and balanced, (ii) that the loads of all 35 kV cables are continuously balanced across the phases and equal to the continuously permissible values, and (iii) that the construction elements of the 35 kV cables which are made from impregnated paper, semi-conducting paper, impregnated jute, and bitumen impregnated jute have the same thermal conductivity.

- To calculate the ampacities of the 110 kV cable line and group of 35 kV cables for their designs outside the hot spot, under the most unfavourable summer conditions and the most common winter conditions; assuming that the surfaces of both cable trenches are covered with grass and neglecting the thermal effects of other underground installations along the entire routes of these cables.
- To calculate the ampacities of the 110 kV cable line and group of 35 kV cables for their designs in the hot spot, under the same environmental conditions; taking into account only the thermal effect of the heating pipeline, which is exploited to the maximum extent throughout the year.
- To develop base cases for winter and summer periods using the FEM-based model associated with the actual cross section of the hot spot [16].
- To assume (i) that both cable trenches are completely filled with thermally stable bedding (TSB) and/or pure quartz sand (PQS) and (ii) that the upper surfaces of both cable trenches have the same radiation properties. The TSB is composed of cement (2%), sand known as Moravac and gravel with fine-grained aggregates of the particles 0–16 mm [16].
- To validate the created FEM-based models using the experimental validation process from [2–4], where it was shown that the ampacities of underground power cables can be increased by means of cool pavements, i.e. surface radiation properties. The experimental validation process is not repeated in this paper.
- To simulate temperature field distributions using the created FEM-based models for six different upper surfaces of both cable trenches.
- To estimate specific investment costs for the considered solutions.
- To compare and discuss the obtained results in order to draw a number of interesting conclusions.

2 FEM-based steady-state thermal models

Figure 1a illustrates the hot spot considered, i.e. the computational domain used for the two base cases. The first base case relates to the following environmental conditions: (i) temperature of the air contacting the earth surface $T_a = 40$ °C; (ii) wind velocity $v_a = 0.22$ m/s; (iii) solar irradiance incident on the earth surface $Q_{S,s} = 1000$ W/m^2; (iv) temperature of referent soil of 20 °C; (v) temperature of the exterior of the heating-pipe duct of 50 °C, along the entire length of the duct when the 110 kV and 35 kV cables are not loaded or at a referent distance from the cable trenches when the 110 kV and 35 kV cables are loaded, and (vi) thermal conductivities of the existing bedding around the 110 kV cable line, existing bedding

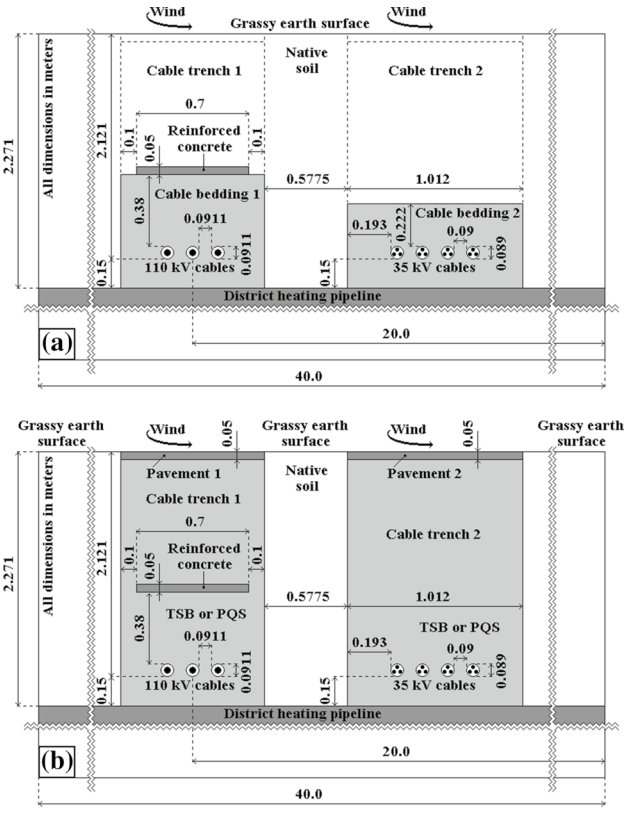

Fig. 1 Presentation of the computational domains for **a** base cases and **b** proposed solutions

around the 35 kV cables and native soil whose values correspond to their dried-out states, i.e. 0.55 W/(m K), 0.326 W/(m K), and approximately 0.4 W/(m K), respectively. According to [4, 16], these conditions represent the most unfavourable summer conditions.

The second base case relates to the most common winter conditions, namely [4]: $T_a = 5$ °C, $v_a = 0.22$ m/s, $Q_{S,s} = 500$ W/m^2, temperature of referent soil of 10 °C, temperature of the exterior of the heating-pipe duct of 50 °C (under the same assumptions as for the most unfavourable summer conditions), and thermal conductivities of the two cable beddings and native soil in the dried-out condition [i.e. 0.55 W/(m K), 0.326 W/(m K), and 0.4 W/(m K)]. The referent soil in both base cases is located below the heating pipeline and its effect is negligible, and the 110 kV and 35 kV cables will be analysed under the stated environmental conditions.

Figure 1b presents the computational domain used for the proposed solutions, where the two cable trenches are completely filled with the same or different bedding materials (TSB, PQS, or their combination) and covered with the same pavements or dry grass. Simulations over the domain shown in Fig. 1b are conducted for the TSB and PQS materials, as well as for the following six surfaces above the 110 kV and 35 kV cables: asphalt coated with cool white coating (the

best case), light bricks, light limestone, concrete blocks, dry grass, and uncoated asphalt (the worst case).

In order to determine the possible ampacities of the 110 kV cable line and group of 35 kV cables, two additional domains showing cross sections of the cable trenches 1 and 2 outside the hot spot are also required. The general requirements that were applied to the design and installation of the 110 kV cable line and the group of four 35 kV cables are presented in Fig. 2a and b, respectively. The external dimensions of these two computational domains are similar to the ones described in [2–4]. In addition to this, the thermal conductivities of the existing bedding around the 110 kV cables, existing bedding around the 35 kV cables, and native soil are the same as the ones in Fig. 1a.

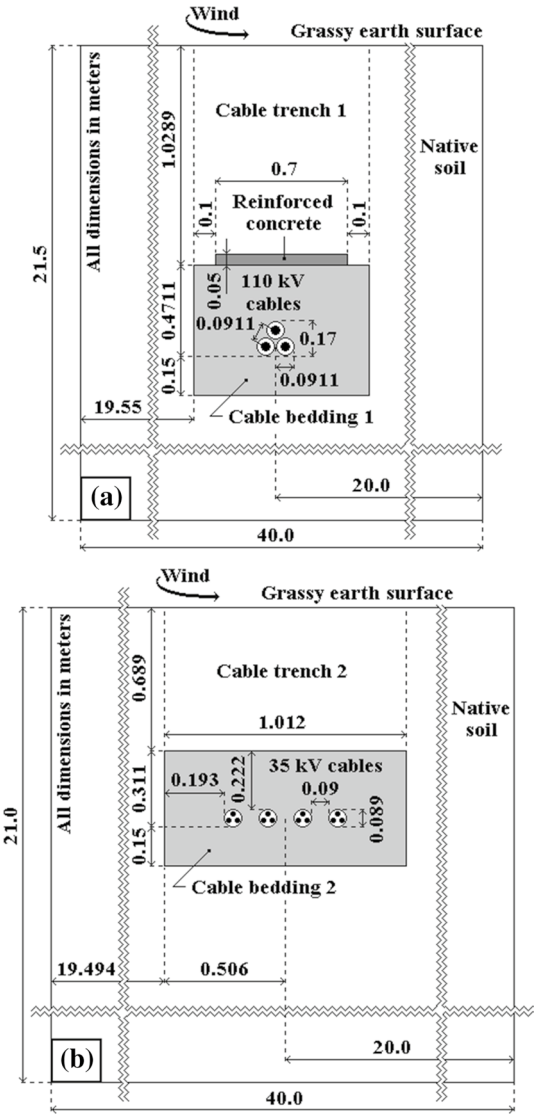

Fig. 2 Presentation of the additional computational domains with **a** 110 kV cable line and **b** group of four 35 kV cables

All the construction elements of the NA2XS(FL)2Y $1 \times 1000/95$ mm^2 64/110 kV and NAEKEBA 3×150 mm^2 20/35 kV cables are described in Figs. 3 and 4, respectively. Also, abbreviations that appear in Fig. 3 relate to the polyethylene (PE), high-density polyethylene (HDPE), and cross-linked polyethylene (XLPE).

For the purposes of simulations using the COMSOL Multiphysics, each of the NA2XS(FL)2Y $1 \times 1000/95$ mm^2 64/110 kV cables is modelled with an equivalent single-core construction composed of the aluminium conductor, XLPE insulation, copper screen, and outer HDPE sheath with outer radii 0.01915 m, 0.04025 m, 0.04165 m, and 0.04555 m, respectively. According to [3, 7, 17], this equivalent single-core construction is created in the following manner: (i) the semi-conducting screens and swelling tapes under the metal screen are added to the block representing the XLPE insulation and (ii) the swelling tapes over the metal screen and water-sealing aluminium layer are modelled with an equivalent metal screen with the thermal conductivity of copper.

For the same purposes, each of the NAEKEBA 3×150 mm^2 20/35 kV cables is modelled with an equivalent three-core construction composed of the aluminium conductors, impregnated paper insulations, separate lead sheaths, impregnated

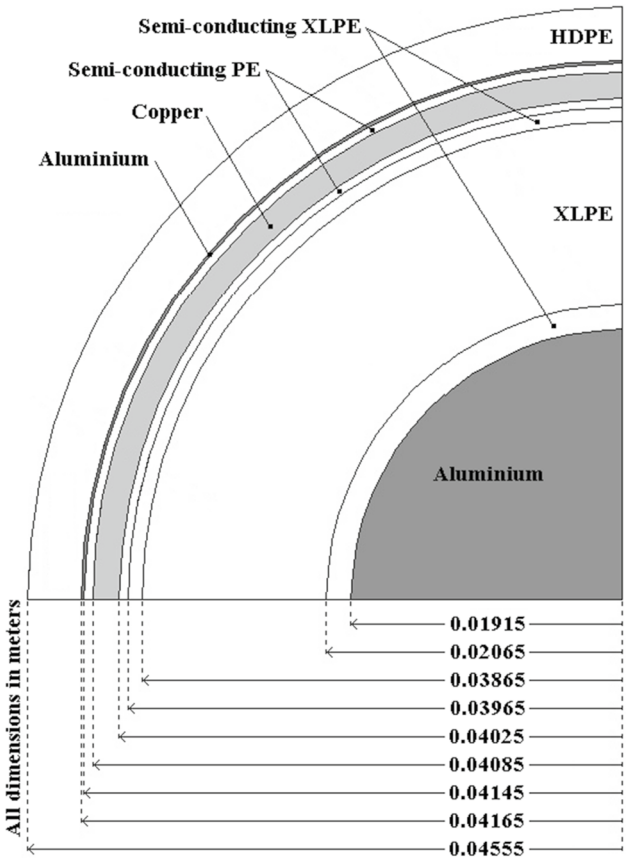

Fig. 3 Dimensions and materials of the construction elements of the NA2XS(FL)2Y $1 \times 1000/95$ mm^2 64/110 kV cable

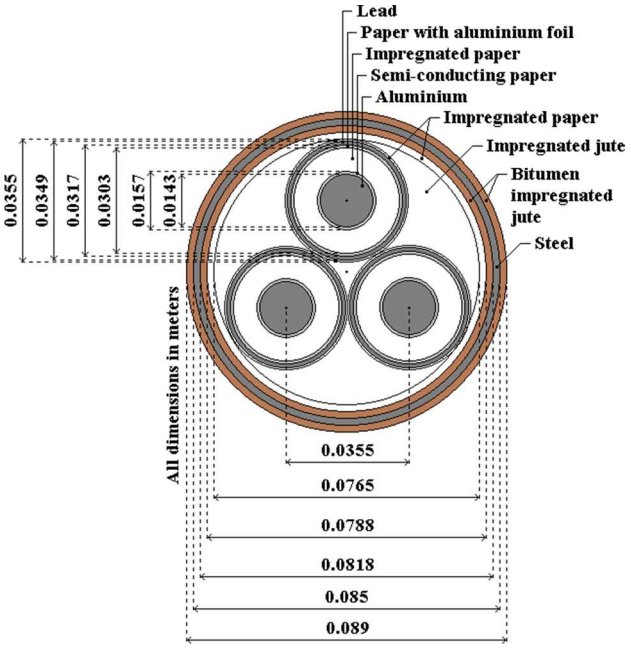

Fig. 4 Dimensions and materials of the construction elements of the NAEKEBA 3×150 mm^2 20/35 kV cable

jute filling, steel armouring, and bitumen impregnated jute serving with outer diameters 0.0143 m, 0.0303 m, 0.0349 m, 0.0818 m, 0.085 m, and 0.089 m, respectively. This equivalent three-core construction is created in the following manner [7, 17]: (i) the semi-conducting conductor screens are added to the blocks representing the impregnated paper insulations; (ii) the insulation screens, i.e. the papers with perforated aluminium foils are added to the blocks representing the separate lead sheaths; and (iii) the impregnated jute filling and two layers of inner protection are modelled with an equivalent filling with the thermal conductivity of impregnated jute.

Table 1 Thermal conductivity of all used materials

Material	k [W/(m K)]
Aluminium	239
Copper	385
Steel	48
Lead	34.5
PE, HDPE, and XLPE	0.286
Compounded jute	0.167
Paper insulation in solid type cables	0.167
Existing bedding around the 110 kV cable line (cable bedding 1)	0.55
Existing bedding around the 35 kV cables (cable bedding 2)	0.326
Native soil	0.4
Thermally stable bedding (TSB), 2000 kg/m^3	1
Pure quartz sand (PQS), 1600 kg/m^3, at 90 °C	5–8.5
Asphalt, 2300 kg/m^3	1.2
Brick, light, solid, 2600 kg/m^3	1
Limestone, light, 2180 kg/m^3	1.5
Concrete block, 2000 kg/m^3	1.3
Reinforced concrete, 2000 kg/m^3	1.16

The governing equation for two-dimensional (2D) FEM-based modelling of steady-state heat transfer in the hot spot has the following form [2–4]:

$$\frac{\partial}{\partial x}\left(k\frac{\partial T}{\partial x}\right)+\frac{\partial}{\partial y}\left(k\frac{\partial T}{\partial y}\right)+Q_{\mathrm{v}}=0, \tag{1}$$

where k is the thermal conductivity in W/(m K); T is the unknown temperature in K; x, y are the Cartesian spatial coordinates in m; and Q_{v} is the volume power of heat sources in W/m^3. The thermal conductivities of all materials appearing in the FEM-based models are listed in Table 1. The governing equation is nonlinear due to the radiation boundary conditions on the earth and pavements' surfaces.

The volume power of heat sources Q_{v} in each conductor of the 110 kV cables and each conductor of the 35 kV cables, having, respectively, a diameter of d_{c}=0.0383 m and d_{c}=0.0143 m and a geometric cross-sectional area of $S'_{\mathrm{c}}=1152.093\cdot10^{-6}$ m^2 and $S'_{\mathrm{c}}=160.606\cdot10^{-6}$ m^2 is

$$Q_{\mathrm{v}}=\frac{R_{\mathrm{ac}}(T_{\mathrm{cp}})}{S'_{\mathrm{c}}}\cdot I^2, \tag{2}$$

where $R_{\mathrm{ac}}(T_{\mathrm{cp}}=90^{\mathrm{o}}\mathrm{C})=40.3772\times10^{-6}$ Ω/m and $R_{\mathrm{ac}}(T_{\mathrm{cp}}=60^{\mathrm{o}}\mathrm{C})=243\times10^{-6}$ Ω/m are the effective conductor resistances to the flow of alternating current (i.e. effective a.c. resistances) per unit length of the 110 kV and 35 kV cables at temperatures T_{cp}=90 °C and T_{cp}=60 °C, respectively, and I is the load current in A. The two effective a.c. resistances take into account the skin and proximity effects, as well as losses in the metal screens or sheaths. However, due to the fact that the 110 kV cables are laid in the flat formation in the hot spot only [16], the effective conductor resistance of the 110 kV cables corresponds to a trefoil formation where the cables are in contact with each other.

Volume powers of heat sources in the cable insulations and metal screens or sheaths of the 110 kV and 35 kV cables are equal to zero due to the following facts [7, 17, 19]: (i) the associated dielectric losses per unit length in each phase of the 110 kV cable line and any 35 kV cable are equal to 0.2583 W/m and 0.1366 W/m, respectively, which are absolutely negligible, (ii) there are no losses in the metal screens of the 110 kV cables because of their cross bonding, and (iii) the effect of heat generated in the lead sheaths of the 35 kV cables is taken into account using the corresponding effective conductor resistance.

The zero heat flux (adiabatic, homogenous, insulation, or symmetry) boundary condition is used to model boundaries

surrounding the left-hand and right-hand sides of the two domains in Fig. 1 and the left-hand, right-hand, and bottom sides of the two domains in Fig. 2 (with regard to the earth surface):

$$k \cdot \frac{\partial T}{\partial n} = 0, \tag{3}$$

where T is the unknown temperature of the corresponding surfaces (model boundaries) in K and n is the length of the normal vector $\vec{n}$ in m.

The edge representing the upper surface of the heating-pipe duct in Fig. 1a and b is modelled with the constant heat flux boundary condition, i.e.

$$k \cdot \frac{\partial T}{\partial n} = -q_0 = -0.94 \text{ W/m}^2, \tag{4}$$

or

$$k \cdot \frac{\partial T}{\partial n} = -q_0 = -8.05 \text{ W/m}^2, \tag{5}$$

where q_0 is the specified heat flux on the upper surface of the heating-pipe duct in W/m^2. In this manner, the thermal effect of the heating pipeline on the 110 kV and 35 kV underground cables is modelled accurately enough for the summer and winter periods. Namely, the boundary conditions (4) and (5) correspond to the summer and winter periods, respectively.

At first glance, the introduction of the boundary conditions (4) and (5) leads to the conclusion that the heating pipeline extends into infinity in the direction of the longitudinal axes of the cables (as shown in Fig. 1). However, according to [16], the external dimension of the heating-pipe duct in the direction of the longitudinal axes of the cables is 1.9 m which is greater than the unit thickness of the three-node triangular elements used in the 2D FEM-based steady-state thermal models. For the International System of Units (SI), the unit thickness of the finite elements equals 1 m [20]. Accordingly, each temperature distribution over the 2D domain in Figs. 1a, b, 2a, or b will be identical to the one over a cross section of the corresponding 3D domain with a length of 1 m in the direction of the longitudinal axes of the cables. By acting in this manner, the upper surface of the heating-pipe duct will not behave as a cooler of the 110 kV and 35 kV cables and its temperature will be equal to 50 °C at a referent distance from the cable trenches.

The heat transfer along the earth and pavements' surfaces is represented by a combination of the following boundary conditions [2–4]:

- The convection boundary condition:

$$k \cdot \frac{\partial T}{\partial n} = h \cdot (T - T_a). \tag{6}$$

- The radiation boundary condition:

$$k \cdot \frac{\partial T}{\partial n} = \varepsilon \cdot \sigma_{SB} \cdot T^4 - \alpha \cdot Q_{S,s}, \tag{7}$$

where T is the unknown surface temperature of the earth or pavements in K, $\alpha = 0.6$ and $\varepsilon = 0.94$ are the solar absorptivity and thermal emissivity for a dry grassy surface, $h = 12.654$ W/(m^2 K) is the heat transfer coefficient due to convection for a dry grassy surface when $v_a = 0.22$ m/s, $h = 8$ W/(m^2 K) for a pavement surface when $v_a = 0.22$ m/s, and $\sigma_{SB} = 5.67 \cdot 10^{-8}$ W/(m^2 K^4) is the Stefan–Boltzmann constant. The coefficients h take into account heat transfer due to free and forced convection between the earth and pavements' surfaces and the ambient air, as well as the effect of evaporation of water from the grassy surfaces. Accordingly, the coefficient h for a grassy surface has a greater value than the one for a pavement surface. This is explained in details in [2–4]. Other values for the coefficients α and ε are given in Table 2. The pavement materials are selected so that their coefficients α and ε are assumed to be equal to the lower bounds of the corresponding ranges of possible values from Table 2.

3 Experimental background and mesh independence tests

The effect of the pavement surface radiation properties (i.e. solar absorptivity and thermal emissivity) on heat transfer between underground power cables and the air contacting the pavement surface above the cables, as well as on the cable ampacity, was validated in [2–4]. In addition, it was shown that this effect is most significant when the cable trench is completely filled with the bedding material. Also, all the numerical results relating to this effect were obtained using the FEM and validated with relevant experiments. More details on the experimental validation can be found in [2–4], which can be considered as an adequate experimental background for this study.

The computational domains from Figs. 1 and 2 were automatically meshed with linear triangular elements.

Table 2 Radiation properties of pavement surfaces and cool white coating

Material or coating	α (–)	ε (–)
Cool white coating	0.15	0.9
Brick, light	0.25–0.36	0.85–0.95
Limestone, light	0.33	0.9–0.93
Concrete block	0.56–0.69	0.94
Asphalt	0.87	0.93

These triangles were interconnected by common nodes and edges, as well as grouped into blocks. In order to show that the steady-state thermal analysis depends on a very small extent on the numbers of nodes and elements, the temperatures at the axes of the conductors of the 110 kV and 35 kV cables were tracked. The numbers of nodes and elements were varied from the ones corresponding to automatic mesh generation to the numbers of nodes and elements corresponding to the first and second mesh refinements. The differences between the temperatures obtained using different meshes were lower than 0.007 °C for all the computational domains considered. Therefore, the changes in temperatures of the conductors of the 110 kV and 35 kV cables could not affect their ampacities to a considerable extent. This means that the independence of the steady-state thermal analysis from the mesh density is ensured using meshes with the numbers of nodes and elements corresponding to automatic mesh generation. These mesh independence tests are performed similarly as described in [21–23]. Table 3 outlines the details on the meshes generated and corresponding mesh independence tests.

4 Results and discussion

Table 4 lists the possible values for the volume powers of heat sources and ampacities of the 110 kV cable line and group of four 35 kV cables calculated for their designs in and outside the hot spot, under the most unfavourable summer conditions and the most common winter conditions. The first and second rows of this table relate to the domain shown in Fig. 1a, i.e. the designs of the cable trenches 1 and 2 in the hot spot. The third and fourth rows of Table 4 relate, respectively, to the designs of the cable trenches 1 and 2 outside the hot spot, i.e. the domains shown in Fig. 2a and b. The ampacities from the first or second row of Table 4 are adjusted by taking into account only the thermal effect of the heating pipeline, i.e. ignoring the effect of heat sources from the adjacent cable trench. Also, the dimensions, materials, and thermal conductivities of the cable beddings 1 and 2 from Fig. 1a remained the same as in [16].

Based on the description of Table 4, it is clear that the considered 110 kV and 35 kV cables can not be loaded at the same time with currents of 414.1 A and 41.2 A in the summer period or with currents of 437.6 A and 46.7 A in the winter period, respectively. This also applies, of course,

Table 3 Details on the meshes generated and corresponding mesh independence tests

Domain	Finite element mesh		Temperature differences
	Automatically generated		
	Number of nodes	Number of elements	°C
Figure 1a or b	14,457	28,765	–
Figure 2a	4527	8969	–
Figure 2b	10,532	20,975	–
After the 1st refinement			
Figure 1a or b	57,678	115,060	< 0.007
Figure 2a	18,022	35,876	< 0.006
Figure 2b	42,038	83,900	< 0.004
After the 2nd refinement			
Figure 1a or b	230,415	460,240	< 0.007
Figure 2a	71,919	143,504	< 0.006
Figure 2b	167,975	335,600	< 0.004

Table 4 Possible values for the volume powers of heat sources and ampacities of the 110 kV cable line and group of 35 kV cables calculated for their designs in and outside the hot spot in the summer and winter periods

Domain	Cables	Radiation properties of the earth surface		T_{cp} (°C)	Results obtained for the most unfavourable summer conditions		Results obtained for the most common winter conditions	
		α (–)	ε (–)		Q_v (W/m^3)	I_{cp} (A)	Q_v (W/m^3)	I_{cp} (A)
Figure 1a	110 kV	0.6	0.94	90	6010	414.1	6710	437.6
Figure 1a	35 kV	0.6	0.94	60	2565	41.2	3300	46.7
Figure 2a	110 kV	0.6	0.94	90	9405	518	17,795	712.6
Figure 2b	35 kV	0.6	0.94	60	6650	66.3	24,075	126.1

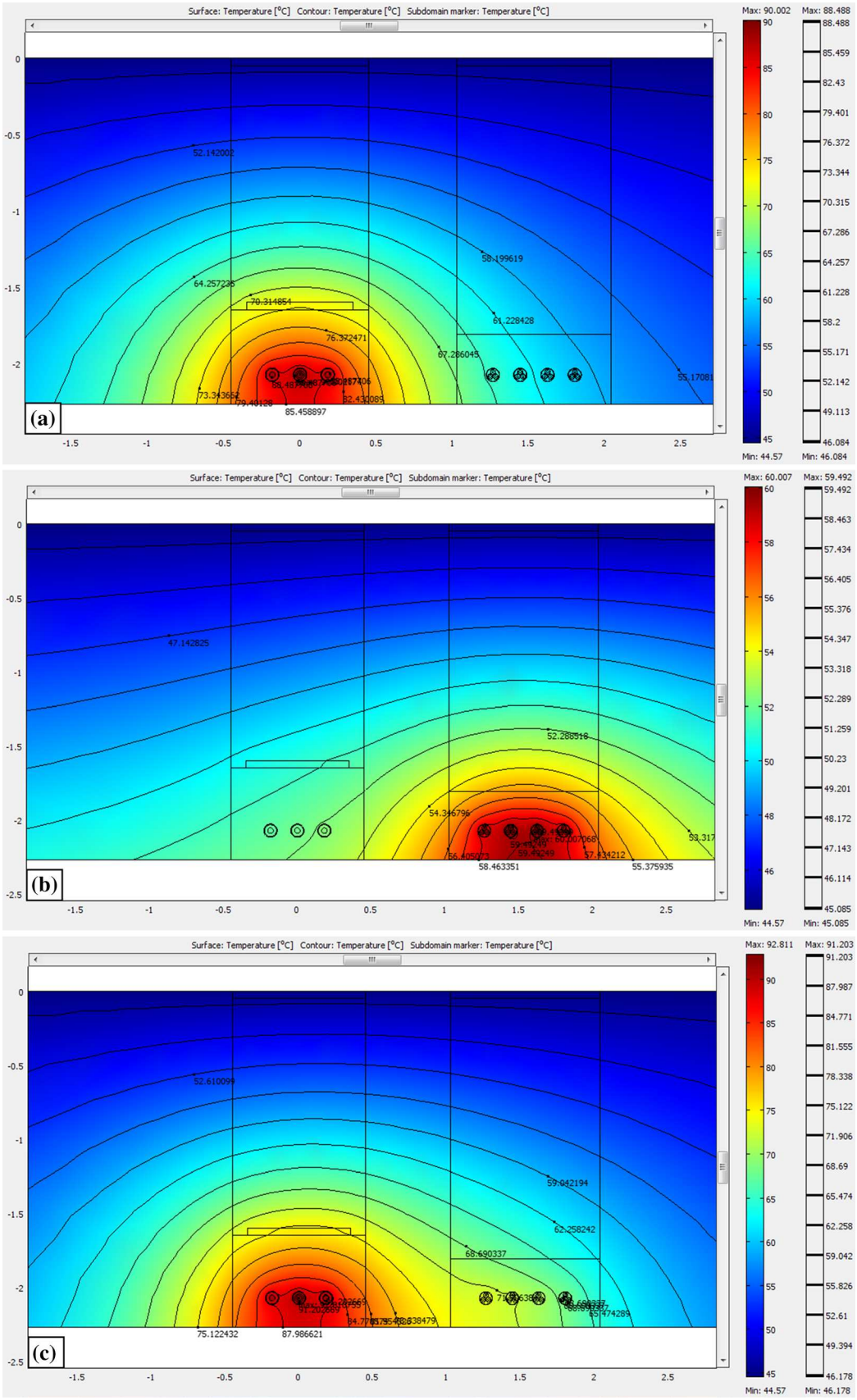
Surface: Temperature [°C] Contour: Temperature [°C] Subdomain marker: Temperature [°C]
Max: 90.002
Min: 44.57
Max: 88.488
Min: 46.084
52.142002
58.199619
64.257236
70.314854
61.228428
76.372471
67.286045
55.17081
73.343664
79.40128
82.430089
85.458897
(a)
Surface: Temperature [°C] Contour: Temperature [°C] Subdomain marker: Temperature [°C]
Max: 60.007
Min: 44.57
Max: 59.492
Min: 45.085
47.142825
52.288518
54.346796
53.317
58.463351
55.375935
(b)
Surface: Temperature [°C] Contour: Temperature [°C] Subdomain marker: Temperature [°C]
Max: 92.811
Min: 44.57
Max: 91.203
Min: 46.178
52.610099
59.042194
62.258242
68.690337
75.122432
87.986621
(c)

◂**Fig. 5** Temperature distribution over the part of the domain in Fig. 1a that presents the cable trenches 1 and 2, obtained for the most unfavourable summer conditions and the following currents of the 110 kV and 35 kV cables: **a** 414.1 A and 0 A, **b** 0 A and 41.2 A, and **c** 414.1 A and 41.2 A, respectively

to each pair of currents from the last two rows of Table 4. Moreover, without some optimisation method, it is not possible to determine the corresponding cable ampacities which take into account the existing thermal environment of the hot spot. In any case, optimal values of the ampacities should be lower than the corresponding ones from the first two rows of Table 4, which itself indicates optimisation is generally not required here.

From the aspect of the thermal effects of underground installations on the cable ampacities, it is interesting to see the temperature distributions over the domain in Fig. 1a for the following cases: (i) the 110 kV cable line is loaded, while the 35 kV cables are not, (ii) the 35 kV cables are loaded, while the 110 kV cable line is not, and (iii) the 110 kV cable line and 35 kV cables are loaded at the same time with the values of currents from the first two rows of Table 4. In addition, the effect of the heating pipeline was introduced by means of the constant heat flux boundary conditions (4) and (5), so that at a referent distance from the cable trenches 1 and 2, as well as in the hot spot when the 110 kV and 35 kV cables are not loaded, the temperature of the exterior of the heating-pipe duct equals 50 °C, regardless of the period of year. The results associated with these cases are shown in Figs. 5 and 6. Figure 5 relates to the most unfavourable summer conditions, while Fig. 6 relates to the most common winter conditions. The simulation results from Figs. 5c and 6c are used as the base cases 1 and 2, respectively.

According to Figs. 5a and 6a, when the 35 kV cables are not loaded, the heating pipeline and 110 kV cable line can increase the temperature of a part of the cable bedding 2 above 60 °C, i.e. above the continuously permissible temperature of the 35 kV cables (T_{cp}= 60 °C). In addition, according to Figs. 5b and 6b, when the 110 kV cable line is not loaded, the heating pipeline and 35 kV cables can increase the temperature of a part of the cable bedding 1 up to 53.3 °C, which is far less than the continuously permissible temperature of the 110 kV cables (T_{cp}= 90 °C). Hence, the thermal effect of the 110 kV cables on the 35 kV cables is much higher than the thermal effect of the 35 kV cables on the 110 kV cables, which is certainly due to the difference between the continuously permissible temperatures of these cables and a relatively small distance between the 110 kV and 35 kV cables.

When all the 110 kV and 35 kV cables are simultaneously loaded with the pairs of currents from the first two rows of Table 4, according to Figs. 5c and 6c, the maximum temperatures of the 110 kV and 35 kV cable conductors are higher than the corresponding continuously permissible temperatures. In these two cases, temperatures in some parts of the cable beddings 1 and 2 are also increased above the corresponding continuously permissible temperatures. However, the increase is much more pronounced in the case of cable bedding 2. For this reason, the thermal conductivities of the TSB and PQS materials are selected in accordance with the continuously permissible temperature of the 110 kV cables. Furthermore, although it is not shown in each of the temperature distributions from Figs. 5 and 6, at reference distances from the cable trench 1 to left and from the cable trench 2 to right, the temperature of the exterior of the heating-pipe duct is 50 °C.

For the purposes of determining what retrofitting solutions should be applied in order to mitigate or exclude the effect of the hot spot on the 110 kV cable line and group of 35 kV cables, three sequences of simulations over the domain in Fig. 1b are performed with the thermal conductivity (k) and surface radiation properties (α and ε) of the asphalt coated with cool white coating, light bricks, light limestone, concrete blocks, TSB or PQS material covered with dry grass, and uncoated asphalt. Bearing in mind the assumptions listed in the introduction, as well as the surface radiation properties of the earth and pavements and the thermal conductivities of the TSB and PQS materials, there is no reason to limit the ampacities of the 110 kV and 35 kV cables to the values lower than the ones corresponding to the designs outside the hot spot shown in, respectively, Fig. 2a and b. Accordingly, it is prescribed that the ampacities of the 110 kV cable line and group of 35 kV cables could be equal to 518 A and 66.3 A for the most unfavourable summer conditions, or 712.6 A and 126.1 A for the most common winter conditions, respectively. These ampacities and the associated volume powers of heat sources were previously labelled as the 'possible ampacities' and the 'possible volume powers of heat sources'.

Temperatures of the most thermally loaded conductors $T_{c,max}$ of the 110 kV cable line and group of 35 kV cables are then estimated for the domain in Fig. 1b, possible ampacities for the most unfavourable summer conditions and the most common winter conditions, different radiation properties of the upper surfaces of the cable trenches, and the following three cases: (i) TSB in both trenches, (ii) TSB in the trench 1 and PQS in the trench 2, and (iii) PQS in both trenches.

The temperatures of the most thermally loaded conductors $T_{c,max}$ of the 110 kV and 35 kV cables obtained for the cases (i), (ii), and (iii) are given in Tables 5, 6 and 7, respectively. In these tables, the currents of the 110 kV cable line or the group of 35 kV cables refer to the ampacities I_{cp} if the temperatures $T_{c,max}$ are equal to or lower than the corresponding continuously permissible temperatures T_{cp} or the

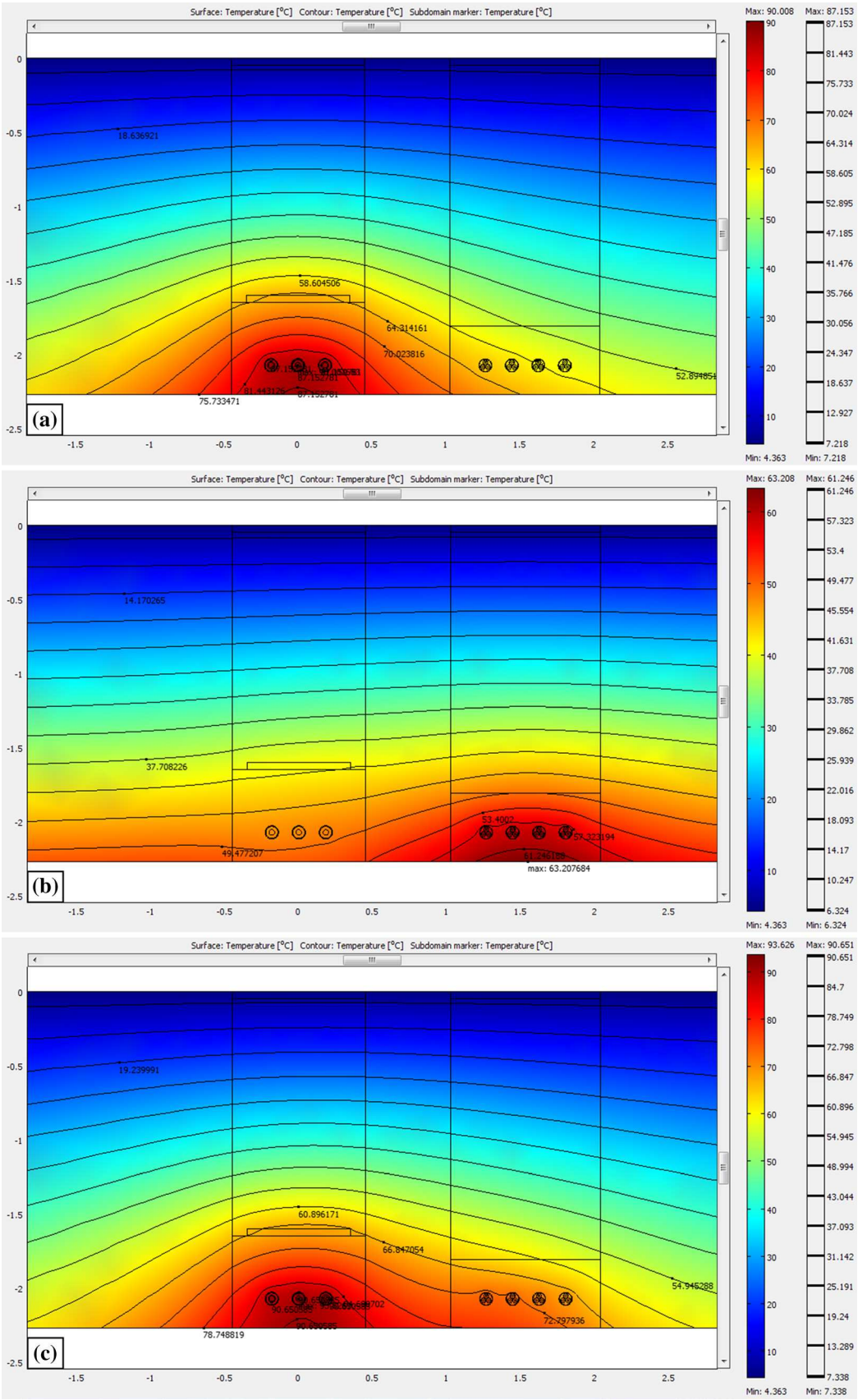
Surface: Temperature [°C] Contour: Temperature [°C] Subdomain marker: Temperature [°C]
Max: 90.008
Min: 4.363
Max: 87.153
Min: 7.218
18.636921
58.604506
64.314161
70.023816
52.894854
75.733471
(a)
Surface: Temperature [°C] Contour: Temperature [°C] Subdomain marker: Temperature [°C]
Max: 63.208
Min: 4.363
Max: 61.246
Min: 6.324
14.170265
37.708226
53.4002
57.323194
49.477207
max: 63.207684
(b)
Surface: Temperature [°C] Contour: Temperature [°C] Subdomain marker: Temperature [°C]
Max: 93.626
Min: 4.363
Max: 90.651
Min: 7.338
19.239991
60.896171
66.847054
54.946288
72.297936
78.748819
(c)

◂**Fig. 6** Temperature distribution over the part of the domain in Fig. 1a that presents the cable trenches 1 and 2, obtained for the most common winter conditions and the following currents of the 110 kV and 35 kV cables: **a** 437.6 A and 0 A, **b** 0 A and 46.7 A, and **c** 437.6 A and 46.7 A, respectively

load currents I if the temperatures $T_{c,max}$ are higher than the corresponding continuously permissible temperatures T_{cp}.

According to Table 5, the ampacities of the 110 kV cable line and group of 35 kV cables in the hot spot can be identical to those referring to the designs outside the hot spot only when the cable trenches 1 and 2 are completely filled with the TSB material in combination with the asphalt coated with cool white coating (the first retrofitting solution). This only applies to the most unfavourable summer conditions. Also, this solution can just be used for mitigating of the hot spot effect on the cable ampacities.

In the cable trench 2, heat sources (i.e. conductors) are more numerous and located closer to each other. This is the main reason for considering the solution where the first cable trench is completely filled with the TSB material and the second one with the PQS material whose thermal conductivity is five times higher than that of the TSB material at 90 °C. The results in Table 6 showed that this solution (the second retrofitting solution) can only be applied to the most unfavourable summer conditions, for all the considered surfaces except for the surface of uncoated asphalt (which is otherwise not a cool pavement). Hence, this solution gives the expected results for all the considered surfaces having absorptivity-to-emissivity ratios below or equal to about 0.6. This is in accordance with the appropriate conclusion from [3]. Furthermore, in this manner, it can be ensured that the group of 35 kV cables can be loaded with the corresponding ampacity under the most common winter conditions, which can not be achieved for the 110 kV cable line.

In addition, a sequence of simulations was also performed with the PQS material in the cable trench 1 and the TSB material in the cable trench 2, assuming that the trenches are completely filled. Because the group of 35 kV cables could not be thermally unloaded in this manner under the most common winter conditions, regardless of the surface radiation properties, results from these simulations are not presented here. In the given case, the thermal unloading of the group of 35 kV cables is achieved only for the most unfavourable summer conditions; namely, for the surface radiation properties of the asphalt coated with cool white coating, light bricks, and light limestone.

Therefore, the second retrofitting solution, according to which the cable trenches 1 and 2 would be completely filled with the different bedding materials, can be used for mitigation of the hot spot effect, but not for its complete and permanent elimination. It is also clear that this solution is better than the one according to which the cable trenches 1 and 2 would be completely filled with the TSB material.

Based on the results from Table 7, the possible ampacities of the 110 kV cable line and group of 35 kV cables can be achieved when the cable trenches (1 and 2) are completely filled with the PQS material (the third retrofitting solution), regardless of the environmental conditions in both summer and winter. This applies to each upper surface of the cable trenches 1 and 2 considered in this study. In particular, this unique solution gives the possibility to increase the ampacity of the 110 kV cable line from 414.1 A to 518 A in summer, and from 437.6 A to 712.6 A in winter. In this manner, the ampacity of the group of four 35 kV cables also increases, from 41.2 A to 66.3 A in summer, and from 46.7 A to 126.1 A in winter. This solution fully and permanently eliminates the hot spot effect.

Before implementing one of the proposed retrofitting solutions in the hot spot, it would also be useful to see temperature distributions over the domain in Fig. 1b for the possible ampacities of the 110 kV cable line and group of 35 kV cables under the most unfavourable summer conditions and the most common winter conditions, PQS material in both cable trenches, and pavements 1 and 2 made from concrete blocks. These temperature distributions correspond to the fourth row of Table 7 and they are presented in Fig. 7a and b. The pavement of concrete blocks is selected as the pavement that is commonly used in practice.

According to Fig. 7a and b, it is evident that the 110 kV cable line and group of 35 kV cables are thermally unloaded under both the most unfavourable summer conditions and the most common winter conditions. Compared with temperature distributions related to the designs of the 110 kV cable line and group of 35 kV cables outside the hot spot, these distributions do not include the isotherms of temperatures between the temperatures of the most thermally loaded conductors of the 110 kV and 35 kV cables and the corresponding continuously permissible temperatures. Therefore, this is another confirmation that the negative effect of the hot spot on the 110 kV and 35 kV cables can be permanently excluded using the third retrofitting solution.

From the economic point of view and considering the possible percentage increases in the ampacities, compared with the solutions proposed in [16], the solution from Fig. 1b, according to which both cable trenches would be completely filled with the PQS material and covered with the same kind of pavement (in order to exclude the negative effect of the hot spot on the 110 kV and 35 kV cables), should be the best and paid back quickly. The current prices of the TSB and PQS materials on the Serbian market are 35.58 EUR/m^3 and 253.4 EUR/m^3, respectively. Hence, the PQS material is about 7 times more expensive than the TSB material. The total amount of bedding material required to permanently exclude the hot spot effect is about 42 m^3,

Table 5 Temperatures of the most thermally loaded conductors of the 110 kV cable line and group of 35 kV cables estimated for the domain in Fig. 1b, possible ampacities corresponding to Fig. 2a and b, TSB material in both trenches, different surface radiation properties, and different environmental conditions

Upper surfaces of the cable trenches	Surface radiation properties		Results obtained for the most unfavourable summer conditions				Results obtained for the most common winter conditions			
			110 kV cables		35 kV cables		110 kV cables		35 kV cables	
	α (–)	ε (–)	I_{cp} or I (A)	$T_{c,max}$ (°C)	I_{cp} or I (A)	$T_{c,max}$ (°C)	I_{cp} or I (A)	$T_{c,max}$ (°C)	I_{cp} or I (A)	$T_{c,max}$ (°C)
Asphalt + coating	0.15	0.9	518	79.35	66.3	58.77	712.6	117.39	126.1	97.51
Brick, light	0.25	0.85	518	84.19	66.3	63.79	712.6	120.38	126.1	100.57
Limestone, light	0.33	0.9	518	86.03	66.3	65.72	712.6	120.97	126.1	101.19
Concrete block	0.56	0.94	518	93.61	66.3	73.59	712.6	125.3	126.1	105.65
Dry grass	0.6	0.94	518	94.23	66.3	74.24	712.6	126.11	126.1	106.49
Asphalt	0.87	0.93	518	104.2	66.3	84.58	712.6	131.64	126.1	112.17

Table 6 Temperatures of the most thermally loaded conductors of the 110 kV cable line and group of 35 kV cables estimated for the domain in Fig. 1b, possible ampacities corresponding to Fig. 2a and b, TSB material in the trench 1, PQS material in the trench 2, different surface radiation properties, and different environmental conditions

Upper surfaces of the cable trenches	Surface radiation properties		Results obtained for the most unfavourable summer conditions				Results obtained for the most common winter conditions			
			110 kV cables		35 kV cables		110 kV cables		35 kV cables	
	α (–)	ε (–)	I_{cp} or I (A)	$T_{c,max}$ (°C)	I_{cp} or I (A)	$T_{c,max}$ (°C)	I_{cp} or I (A)	$T_{c,max}$ (°C)	I_{cp} or I (A)	$T_{c,max}$ (°C)
Asphalt + coating	0.15	0.9	518	70.69	66.3	36.74	712.6	95.71	126.1	36.05
Brick, light	0.25	0.85	518	76.31	66.3	43.48	712.6	99.22	126.1	40.31
Limestone, light	0.33	0.9	518	78.39	66.3	45.89	712.6	99.76	126.1	40.77
Concrete block	0.56	0.94	518	87.16	66.3	56.38	712.6	104.79	126.1	46.79
Dry grass	0.6	0.94	518	87.56	66.3	56.63	712.6	104.6	126.1	45.76
Asphalt	0.87	0.93	518	99.44	66.3	71.05	712.6	112.12	126.1	55.54

Table 7 Temperatures of the most thermally loaded conductors of the 110 kV cable line and group of 35 kV cables estimated for the domain in Fig. 1b, possible ampacities corresponding to Fig. 2a and b, PQS material in both trenches, different surface radiation properties, and different environmental conditions

Upper surfaces of the cable trenches	Surface radiation properties		Results obtained for the most unfavourable summer conditions				Results obtained for the most common winter conditions			
			110 kV cables		35 kV cables		110 kV cables		35 kV cables	
	α (–)	ε (–)	I_{cp} or I (A)	$T_{c,max}$ (°C)	I_{cp} or I (A)	$T_{c,max}$ (°C)	I_{cp} or I (A)	$T_{c,max}$ (°C)	I_{cp} or I (A)	$T_{c,max}$ (°C)
Asphalt + coating	0.15	0.9	518	44.46	66.3	32.98	712.6	40.64	126.1	28.14
Brick, light	0.25	0.85	518	51.3	66.3	39.95	712.6	44.94	126.1	32.5
Limestone, light	0.33	0.9	518	53.7	66.3	42.49	712.6	45.46	126.1	33.1
Concrete block	0.56	0.94	518	64.34	66.3	53.39	712.6	51.55	126.1	39.32
Dry grass	0.6	0.94	518	64.48	66.3	53.7	712.6	50.56	126.1	38.49
Asphalt	0.87	0.93	518	79.22	66.3	68.64	712.6	60.42	126.1	48.4

which means that the total price for the required PQS material would be approximately equal to the price of only one 110 kV cable joint including installation [16].

In addition, specific investment costs for each of the considered solutions are approximately at the same level. This can best be seen from Table 8, which provides the results of the techno-economic analysis carried out for the first rows of Tables 5 and 7. In each of these two cases, the same bedding material is applied in both trenches and the pavements above the 110 kV and 35 kV cables are made from

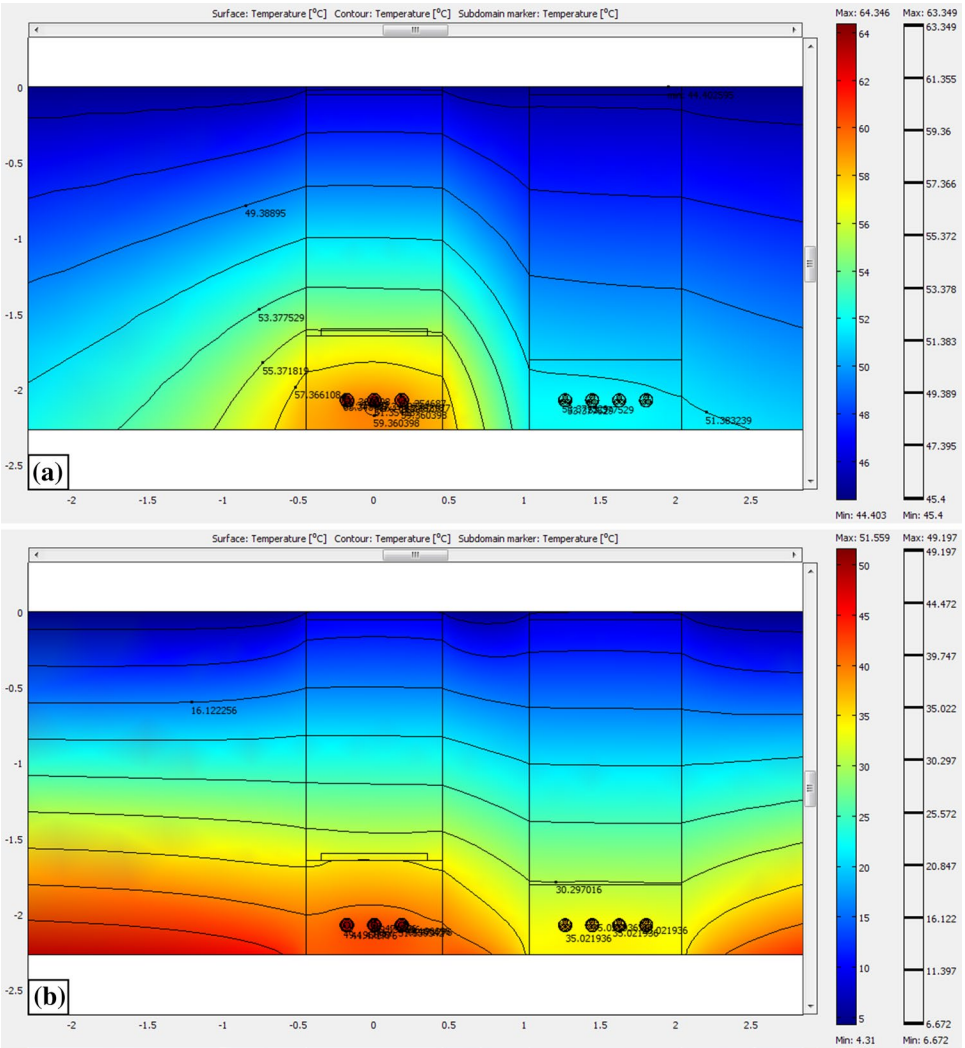

Fig. 7 Temperature distribution over the part of the domain in Fig. 1b that presents the trenches 1 and 2, obtained for the ampacities of the 110 kV and 35 kV cables corresponding to Fig. 2a and b, PQS material in both trenches, and pavements 1 and 2 made from concrete blocks, under **a** the most unfavourable summer conditions and **b** the most common winter conditions

asphalt with white-coated surface. Moreover, the specific investment costs for retrofitting solutions are defined as the ratio of the overall investment costs of the retrofitting solution (without initial costs) and the sum of maximum possible increases in ampacities of all 110 kV and 35 kV cable conductors. According to Tables 4, 5 and 7, the maximum possible increases in ampacities of 110 kV and 35 kV cable conductors have, respectively, the following values: 103.9 A and 25.1 A for the case when the existing cable beddings are replaced with the TSB material, and 275 A and 79.4 A for the case when the existing cable beddings are replaced with the PQS material. Accordingly, the corresponding overall investment costs, sum of maximum possible increases in ampacities of all (110 kV and 35 kV) cable conductors, and specific investment costs are, respectively, 4034.48 EUR, $3 \times 103.9 + 12 \times 25.1 = 612.9$ A, and $4034.48/612.9 = 6.58$ EUR/A—for the first retrofitting solution and 13182.92 EUR, $3 \times 275 + 12 \times 79.4 = 1777.8$ A, and $13182.92/1777.8 = 7.42$ EUR/A—for the third retrofitting solution.

Therefore, it is economically justified to avoid the retrofitting solutions that would only mitigate the hot spot effect (such as the solutions for which the simulation results are presented in Tables 5 and 6) or the overall corrective solution from [16] (which includes the cutting of cables, installation of six 110 kV cable joints, etc.). As far as prices, exploitation, and maintenance of cool pavements are concerned, more information can be found in [1–5].

5 Conclusions

The conclusions that can be drawn from the presented results and discussion are as follows:

- The third retrofitting solution, according to which both cable trenches would be completely filled with the PQS material and covered with the same cool pavement (or dry grass) in the hot spot, gives the possibility to increase the ampacities of the 110 kV cable line and group of four

Table 8 Comparison of specific investment costs obtained for the cases in which the same bedding material is applied in both trenches and in which the pavements are made from asphalt with white-coated surface

Solution	Material, labour and machinery	Current price	Amount	Total
Common for both solutions	Coating + installation	7.3 €/m^2	19 m^2	138.7 €
	Asphalt	17.5 €/m^2	19 m^2	332.5 €
	Soil excavation	7.38 €/m^3	42 m^3	309.96 €
	Bedding regression with tamping	3.67 €/m^3	42 m^3	154.14 €
	Trench timbering	8.02 €/m^2	91 m^2	729.82 €
	Soil transport	7.5 €/m^3	42 m^3	315 €
	Use of machinery	35 €/h	16 h	560 €
Replacing existing cable beddings with TSB	TSB	35.58 €/m^3	42 m^3	1494.36 €
	Overall investment costs (without initial costs)			4034.48 €
	Sum of maximum possible increases in ampacities of all cable conductors			612.9 A
	Specific investment costs			6.58 €/A
Replacing existing cable beddings with PQS	PQS	253.4 €/m^3	42 m^3	10,642.8 €
	Overall investment costs (without initial costs)			13,182.92 €
	Sum of maximum possible increases in ampacities of all cable conductors			1777.8 A
	Specific investment costs			7.42 €/A

35 kV cables up to 25.1% and 60.9% for the most unfavourable summer conditions, and up to 62.8% and 170% for the most common winter conditions, respectively.

- In accordance with the temperature distributions in Figs. 5c and 6c (i.e. the base cases), the obtained values for the percentage increases in the cable ampacities do not represent maximum values which can be achieved. Namely, the ampacities of the 110 kV and 35 kV cables should be lower than 414.1 A and 41.2 A in the summer period, and lower than 437.6 A and 46.7 A in the winter period, respectively. This is supported by the fact that the temperatures of the most thermally loaded conductors of the 110 kV cable line and the group of four 35 kV cables in Figs. 5c and 6c are higher than the corresponding continuously permissible temperatures.
- The first and second retrofitting solutions can be used for mitigation of the negative thermal effect of the hot spot on the ampacities of the 110 kV cable line and group of four 35 kV cables, while the third one permanently eliminates this negative effect.
- According to the relevant literature, the application of a cool pavement in combination with cable trenches that are completely filled with the PQS material in order to eliminate the negative thermal effect of the hot spot on the cable ampacities would be a novelty in the field of power cable engineering.
- It was successfully demonstrated that the solutions similar to the third retrofitting solution can be used for full and permanent elimination of any hot spot along the routes of underground power cables, regardless of their voltage levels.
- Based on the specific investment costs obtained, it is clear that the third retrofitting solution is not expensive, it would result in significant financial benefits and it would be quickly paid back.
- It is shown how the temperature of the exterior of the heating-pipe duct, at a referent distance from the hot spot, can be set to a standard value of 50 °C using the constant heat flux boundary condition during different periods of the year.
- It was found that, in close proximity of the 110 kV and 35 kV cables at the hot spot, the temperatures of the cable beddings may be somewhat higher than the corresponding continuously permissible temperatures.

The proposed solutions can generally be used for all types of hot spots, as well as for the general requirements for the design and installation of underground power cables outside the hot spots. Controlling the thermal environment of underground power cables in the proposed manner can also increase their dynamic ampacities. Moreover, the positive effects on the cable ampacities similar to those associated with any cool pavement can also be achieved by a hydronic asphalt pavement system. Finally, these two topics might be the subjects of future studies for research papers.

Acknowledgements This paper was based on research conducted within the project TR33046 funded by the Ministry of Education, Science, and Technological Development of the Republic of Serbia. Also, the authors would like to thank Aleksandra D. Kuč for her technical assistance.

References

1. Klimenta D, Jevtić M, Klimenta J, Perović B (2018) A review on new methods for increasing the ampacity of underground power cables: cool and photovoltaic pavements. In Proceedings of the 6th international conference on renewable electrical power sources (6th ICREPS), pp 15–21
2. Klimenta D, Perović B, Klimenta J, Jevtić M, Milovanović M, Krstić I (2018) Modelling the thermal effect of solar radiation on the ampacity of a low voltage underground cable. Int J Therm Sci 134:507–516
3. Klimenta D, Perović B, Klimenta J, Jevtić M, Milovanović M, Krstić I (2018) Controlling the thermal environment of underground cable lines using the pavement surface radiation properties. IET Gener Transm Distrib 12(12):2968–2976
4. Klimenta DO, Perović BD, Klimenta TLJ, Jevtić MM, Milovanović MJ, Krstić ID (2018) Controlling the thermal environment of underground power cables adjacent to heating pipeline using the pavement surface radiation properties. Therm Sci 22(6):2625–2640
5. Klimenta D, Jevtić M, Klimenta J, Perović B (2018) The effect of solar radiation on the ampacity of an underground cable with XLPE insulation. In Proceedings of the 4th virtual international conference on science, technology and management in energy (eNergetics 2018), pp 197–204
6. Klimenta D, Jevtić M, Milovanović M (2018) Comparing the effects of solar heating on low voltage underground cables with PVC and XLPE insulations. In: Proceedings of the 47th international scientific forum "Week of Science SPbPU"-2018, Part 2, pp 24–26
7. IEC (2014) IEC Standard Electric Cables-Calculation of the Current Rating-Part 1-1: Current Rating Equations (100% Load Factor) and Calculation of Losses-General, 2.1 edn. IEC 60287-1-1:2006 + AMD1:2014 CSV
8. IEC (2003) IEC technical report electric cables-calculations for current ratings-finite element method, 1st edn. IEC TR 62095:2003
9. Anders GJ (2005) Rating of electric power cables in unfavorable thermal environment, 1st edn. Wiley, Hoboken
10. Nahman J, Tanaskovic M (2011) Evaluation of the loading capacity of a pair of three-phase high voltage cable systems using the finite-element method. Electr Power Syst Res 81(7):1550–1555
11. Nahman J, Tanaskovic M (2013) Calculation of the ampacity of high voltage cables by accounting for radiation and solar heating effects using FEM. Int Trans Electr Energy Syst 23(3):301–314
12. Nahman J, Tanaskovic M (2018) Calculation of the loading capacity of high voltage cables laid in close proximity to heat pipelines using iterative finite-element method. Int J Electr Power Energy Syst 103:310–316
13. Terracciano M, Purushothaman S, de León F, Farahani AV (2012) Thermal analysis of cables in unfilled troughs: Investigation of the IEC standard and a methodical approach for cable rating. IEEE Trans Power Deliv 27(3):1423–1431
14. Yang L, Qiu W, Huang J, Hao Y, Fu M, Hou S, Li L (2018) Comparison of conductor-temperature calculations based on different radial-position-temperature detections for high-voltage power cable. Energies 11(117):1–17
15. Lindström L (2011) Evaluating impact on ampacity according to IEC-60287 regarding thermally unfavourable placement of power cables. Masters' Degree Project, Royal Institute of Technology (KTH), Stockholm, Sweden, XR-EE-ETK 2011:009
16. Klimenta D, Nikolajević S, Sredojević M (2007) Controlling the thermal environment in hot spots of buried power cables. Eur Trans Electr Power 17(5):427–449
17. Klimenta D, Perovic B, Jevtic M, Radosavljevic J, Arsic N (2014) A thermal FEM-based procedure for the design of energy-efficient underground cable lines. Human Sci Univ J Tech 10:162–188
18. COMSOL (2012) Heat transfer module user's guide. Version 4:3
19. Heinhold L (1990) Power cables and their application-Part 1, Third revised edn. Siemens Aktiengesellschaft, Berlin
20. Huebner KH, Dewhirst DL, Smith DE, Byrom TG (2001) The finite element method for engineers, 4th edn. Wiley, New York
21. Salata F, Nardecchia F, Gugliermetti F, de Lieto Vollaro A (2016) How thermal conductivity of excavation materials affects the behavior of underground power cables. Appl Therm Eng 100:528–537
22. Salata F, Nardecchia F, de Lieto Vollaro A, Gugliermetti F (2015) Underground electric cables a correct evaluation of the soil thermal resistance. Appl Therm Eng 78:268–277
23. Salata F, de Lieto Vollaro A, de Lieto Vollaro R (2015) A model for the evaluation of heat loss from underground cables in non-uniform soil to optimize the system design. Therm Sci 19(2):461–474